SUPPLEMENTARY METHODS

Morphological and structural analysis of pKECM

After fixation with 2.5 % glutaraldehyde dehydration in a graded ethanol series, pKECM structure was analyzed by Scanning Electron Microscopy (SEM; JSM-6010 LV, JEOL, Japan). Samples were sputter coated with gold (coater 108 A, Cressington, United States) prior to examination. Micrographs were obtained at an accelerating voltage of 10 kV. The infrared spectra of pKECM before and after sterilization was analyzed by Attenuated total reflection-Fourier transform infrared spectroscopy (ATR-FITR, IRPrestige 21, Shimadzu), with a spectral range of 500-3000 cm^{-1} in reflection mode to characterize the composition and molecular conformation of the pKECM. Thermal properties of the pKECM substrates before and after sterilization were characterized by differential scanning calorimetry (DSC, Q100, TA Instruments). Approximately 2 mg of sterile and non-sterile pKECM were transferred into an aluminum pan and the sample was scanned with a modulated heating method. First, pKECM was heated until 250 °C at a heating rate of 10 °C min^{-1} and then cooled down to 10 °C. The sample chamber was purged with nitrogen at a flow rate of 50 mL h^{-1}.

Histological and biochemical analysis of pKECM

pKECM substrate was assessed by Hematoxylin & Eosin (H&E) and Masson's Trichrome (MT) stainings of frozen sections. The samples were fixed for 30 min with 10 % neutral-buffered formalin before being embedded in OCT compound (Bio-optica). After this, they were snap-freezed in liquid nitrogen and cut into 10 μm sections using a cryostat. Sections were stained with working solutions of H&E and a MT kit according to manufacturer's instructions (Bio-optica), dehydrated through a series of ethanol and mounted. For the detection of dsDNA, pKECM was digested for 2 h at 56 °C with proteinase K and the remaining DNA extraction was performed using DNeasy blood and tissue kit (Qiagen) according to manufacturer's instructions. The digested samples were

quantified using Quanti-iT PicoGreen dsDNA assay kit (Invitrogen) according to the manufacturer's protocol. Values were extrapolated using a standard curve of dsDNA and sample fluorescence was read in a microplate reader (excitation: 485/20 nm; emission: 530/25 nm).

Characterization and relative quantification of protein composition by nano-liquid chromatography–tandem mass spectrometry (nanoLC- MS/MS)

Each sample was reduced and alkylated and processed for proteomics analysis following the solid-phase-enhanced sample-preparation (SP3) protocol as described in PMID30464214.[1] Enzymatic digestion was performed with Trypsin/LysC (2 µg) overnight at 37 ºC at 1000 rpm.

Protein identification and quantitation was performed by nanoLC-MS/MS. This equipment is composed by an Ultimate 3000 liquid chromatography system coupled to a Q-Exactive Hybrid Quadrupole-Orbitrap mass spectrometer (Thermo Scientific, Bremen, Germany). Samples were loaded onto a trapping cartridge (Acclaim PepMap C18 100Å, 5 mm x 300 µm i.d., 160454, Thermo Scientific) in a mobile phase of 2 % acetonitrile (ACN), 0.1% formic acid (FA) at 10 µL min-1. After 3 min loading, the trap column was switched in-line to a 50 cm by 75 µm inner diameter EASY-Spray column (ES803, PepMap RSLC, C18, 2 µm, Thermo Scientific, Bremen, Germany) at 250 nL min-1. Separation was generated by mixing A: 0.1% FA, and B: 80 % ACN, with the following gradient: 5 min (2.5 % B to 10 % B), 120 min (10 % B to 30 % B), 20 min (30 % B to 50 % B), 5 min (50 % B to 99 % B) and 10 min (hold 99 % B). Subsequently, the column was equilibrated with 2.5 % B for 17 min. Data acquisition was controlled by Xcalibur 4.0 and Tune 2.9 software (Thermo Scientific, Bremen, Germany).

The mass spectrometer was operated in data-dependent (dd) positive acquisition mode alternating between a full scan (m/z 380-1580) and subsequent HCD MS/MS of the 10 most intense peaks from full scan (normalized collision energy of 27 %). ESI spray voltage was 1.9 kV. Global settings: use lock masses best (m/z 445.12003), lock mass injection Full MS, chrom. peak width (FWHM) 15 s. Full scan settings: 70 k resolution (m/z 200), AGC target 3E6, maximum injection

time 120 ms. dd settings: minimum AGC target 8E3, intensity threshold 7.3E4, charge exclusion: unassigned, 1, 8, > 8, peptide match preferred, exclude isotopes on, dynamic exclusion 45vs. MS2 settings: microscans 1, resolution 35 k (m/z 200), AGC target 2E5, maximum injection time 110 ms, isolation window 2.0 m/z, isolation offset 0.0 m/z, spectrum data type profile.

The raw data was processed using Proteome Discoverer 2.4.0.305 software (Thermo Scientific) and searched against the UniProt database for the Sus scrofa Proteome 2019_11. The Sequest HT search engine was used to identify tryptic peptides. The ion mass tolerance was 10 ppm for precursor ions and 0.02 Da for fragment ions. Maximum allowed missing cleavage sites was set 2. Cysteine carbamidomethylation was defined as constant modification. Methionine oxidation and protein N-terminus acetylation were defined as variable modifications. Peptide confidence was set to high. The processing node Percolator was enabled with the following settings: maximum delta Cn 0.05; decoy database search target FDR 1 %, validation based on q-value. Protein label free quantitation was performed with the Minora feature detector node at the consensus step. Precursor ions quantification was performing at the processing step with the following parameters: unique plus razor peptides were considered for quantification, precursor abundance was based on intensity and normalization was based on total peptide amount.

The total number of proteins identified in each fraction was obtained by filtering peptide identifications at > 95.0 % confidence interval with at least two peptides per protein. Gene ontology analysis (GO) was performed manually using AmiGO online platform.[2,3] Following categorization, non-ECM proteins were excluded to perform graphical analysis. Coefficient of variation (CV) values were calculated by dividing standard deviation by mean values of the ECM proteins identified on each kidney sample. The mass spectrometry proteomics data have been deposited to the ProteomeXchange Consortium via the PRIDE [4] partner repository with the dataset identifier PXD019122.

Isolation and characterization of human renal progenitor cells (hRPC)

Human kidney fragments were obtained in agreement with the Ethical Committee on human experimentation of the Azienda Ospedaliero-Universitaria Careggi, Florence, Italy. All subjects gave their informed consent for inclusion before they participated in the study. The study was conducted in accordance with the Declaration of Helsinki, and the protocol was approved by the Ethics Committee on Human Experimentation of the Azienda Ospedaliero-Universitaria Careggi, Florence, Italy (project identification code 2015/0009082 from 25/03/2015). Human RPCs were obtained and cultured as previously described,[5] with minor modifications. Briefly, we minced the cortex and we performed an enzymatic digestion with collagenase solution type IV 750 U mL^{-1} (Sigma Aldrich) in PBS for 45 min at 37 °C. After digestion, we filtered the solution by a standard sieving technique through graded mesh screens (60 and 80 mesh). Subsequently, we performed red blood cell lysis by incubating with lysis buffer (NH4Cl 0.087 %) for 4 min at 37 °C. The cellular suspension was collected, washed and plated on petri dish containing complete medium. The medium is composed by Microvascular Endothelial Cell Growth Medium (EGM™-MV, Lonza) supplemented with 20 % HyClone™ Fetal Bovine Serum (FBS, GE Healthcare). After 4 to 5 days of culture, cells that adhered to the plate were subcultured. Cultures were checked for simultaneous expression of CD133 and CD24 by flow cytometry, according to previously published methods for characterizing hRPC.[6] For the analysis, total hRPCs population was gated on a forward scatter (FSC)/side scatter (SSC) plot and dead cells were excluded by Propidium Iodide (PI) staining. Live cells (PI negative) were gated for CD133 and CD24 expression. Only cells between passage 1-3 and expressing > 90 % CD24/CD133 double positivity were used in this study.

REFERENCES

1 C. S. Hughes, S. Moggridge, T. Müller, P. H. Sorensen, G. B. Morin and J. Krijgsveld, *Nat. Protoc.*, , DOI:10.1038/s41596-018-0082-x.

2 S. Carbon, A. Ireland, C. J. Mungall, S. Shu, B. Marshall, S. Lewis, J. Lomax, C. Mungall, B. Hitz, R. Balakrishnan, M. Dolan, V. Wood, E. Hong and P. Gaudet, *Bioinformatics*, , DOI:10.1093/bioinformatics/btn615.

3 S. Carbon, E. Douglass, N. Dunn, B. Good, N. L. Harris, S. E. Lewis, C. J. Mungall, S. Basu, R. L. Chisholm, R. J. Dodson, E. Hartline, P. Fey, P. D. Thomas, L. P. Albou, D. Ebert, M. J. Kesling, H. Mi, A. Muruganujan, X. Huang, S. Poudel, T. Mushayahama, J. C. Hu, S. A. LaBonte, D. A. Siegele, G. Antonazzo, H. Attrill, N. H. Brown, S. Fexova, P. Garapati, T. E. M. Jones, S. J. Marygold, G. H. Millburn, A. J. Rey, V. Trovisco, G. Dos Santos, D. B. Emmert, K. Falls, P. Zhou, J. L. Goodman, V. B. Strelets, J. Thurmond, M. Courtot, D. S. Osumi, H. Parkinson, P. Roncaglia, M. L. Acencio, M. Kuiper, A. Lreid, C. Logie, R. C. Lovering, R. P. Huntley, P. Denny, N. H. Campbell, B. Kramarz, V. Acquaah, S. H. Ahmad, H. Chen, J. H. Rawson, M. C. Chibucos, M. Giglio, S. Nadendla, R. Tauber, M. J. Duesbury, N. T. Del, B. H. M. Meldal, L. Perfetto, P. Porras, S. Orchard, A. Shrivastava, Z. Xie, H. Y. Chang, R. D. Finn, A. L. Mitchell, N. D. Rawlings, L. Richardson, A. Sangrador-Vegas, J. A. Blake, K. R. Christie, M. E. Dolan, H. J. Drabkin, D. P. Hill, L. Ni, D. Sitnikov, M. A. Harris, S. G. Oliver, K. Rutherford, V. Wood, J. Hayles, J. Bahler, A. Lock, E. R. Bolton, J. De Pons, M. Dwinell, G. T. Hayman, S. J. F. Laulederkind, M. Shimoyama, M. Tutaj, S. J. Wang, P. D'Eustachio, L. Matthews, J. P. Balhoff, S. A. Aleksander, G. Binkley, B. L. Dunn, J. M. Cherry, S. R. Engel, F. Gondwe, K. Karra, K. A. MacPherson, S. R. Miyasato, R. S. Nash, P. C. Ng, T. K. Sheppard, A. Shrivatsav Vp, M. Simison, M. S. Skrzypek, S. Weng, E. D. Wong, M. Feuermann, P. Gaudet, E. Bakker, T. Z. Berardini, L. Reiser, S. Subramaniam, E. Huala, C. Arighi, A. Auchincloss, K. Axelsen, G. P. Argoud, A. Bateman, B. Bely, M. C. Blatter, E. Boutet, L. Breuza, A. Bridge, R. Britto, H. Bye-A-Jee, C. Casals-Casas, E. Coudert, A. Estreicher, L. Famiglietti, P. Garmiri, G. Georghiou, A. Gos, N. Gruaz-Gumowski, E. Hatton-Ellis, U. Hinz, C. Hulo, A. Ignatchenko, F. Jungo, G. Keller, K. Laiho, P. Lemercier, D. Lieberherr, Y. Lussi, A. Mac-Dougall, M. Magrane, M. J. Martin, P. Masson, D. A. Natale, N. N. Hyka, I. Pedruzzi, K. Pichler, S. Poux, C. Rivoire, M. Rodriguez-Lopez, T. Sawford, E. Speretta, A. Shypitsyna, A. Stutz, S. Sundaram, M. Tognolli, N. Tyagi, K. Warner, R. Zaru, C. Wu, J. Chan, J. Cho, S. Gao, C. Grove, M. C. Harrison, K. Howe, R. Lee, J. Mendel, H. M. Muller, D. Raciti, K. Van Auken, M. Berriman, L. Stein, P. W. Sternberg, D. Howe, S. Toro and M. Westerfield, *Nucleic Acids Res.*, , DOI:10.1093/nar/gky1055.

4 Y. Perez-Riverol, A. Csordas, J. Bai, M. Bernal-Llinares, S. Hewapathirana, D. J. Kundu, A. Inuganti, J. Griss, G. Mayer, M. Eisenacher, E. Pérez, J. Uszkoreit, J. Pfeuffer, T. Sachsenberg, Ş. Yilmaz, S. Tiwary, J. Cox, E. Audain, M. Walzer, A. F. Jarnuczak, T. Ternent, A. Brazma and J. A. Vizcaíno, *Nucleic Acids Res.*, , DOI:10.1093/nar/gky1106.

5 C. Sagrinati, G. S. Netti, B. Mazzinghi, E. Lazzeri, F. Liotta, F. Frosali, E. Ronconi, C. Meini, M. Gacci, R. Squecco, M. Carini, L. Gesualdo, F. Francini, E. Maggi, F. Annunziato, L. Lasagni, M. Serio, S. Romagnani and P. Romagnani, *J. Am. Soc. Nephrol.*, 2006, **17**, 2443–2456.

6 M. L. Angelotti, E. Ronconi, L. Ballerini, A. Peired, B. Mazzinghi, C. Sagrinati, E. Parente, M. Gacci, M. Carini, M. Rotondi, A. B. Fogo, E. Lazzeri, L. Lasagni and P. Romagnani, *Stem Cells*, 2012, **30**, 1714–1725.

SUPPLEMENTARY FIGURES AND TABLES

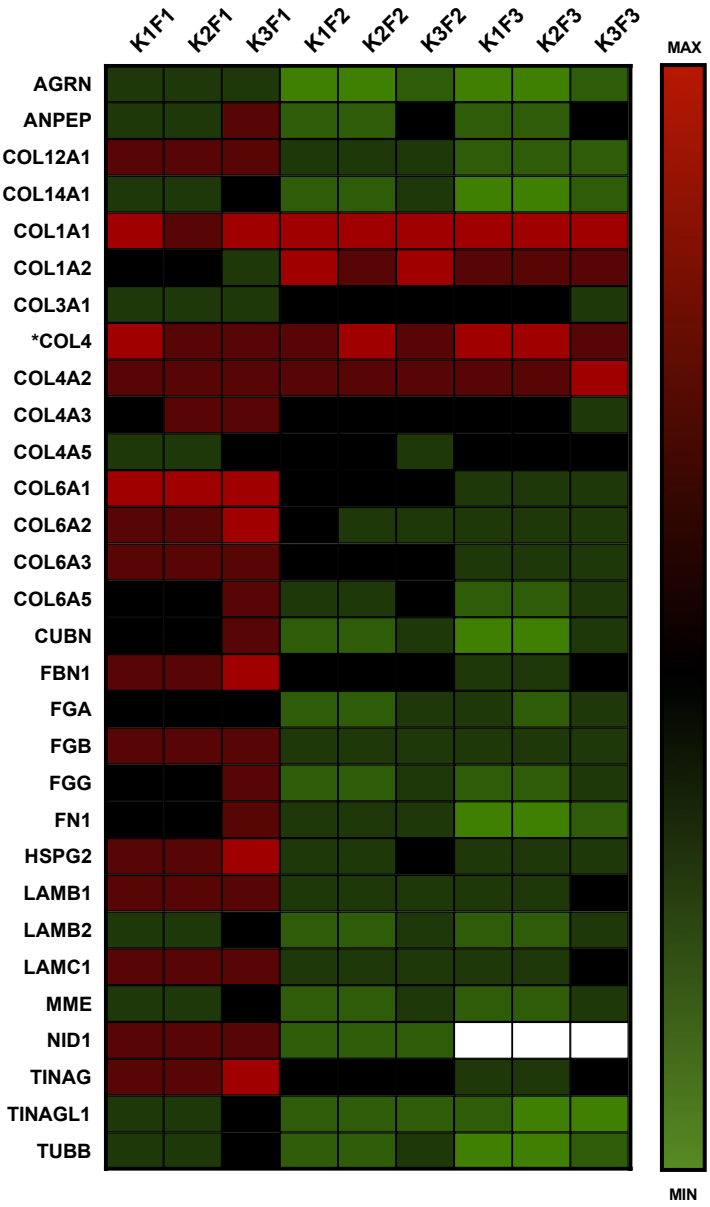

Figure S1 – Quantitative proteomic analysis of the 30 most abundant proteins on decellularized porcine matrix. Heat map representing the absolute abundance per each fraction (F - detailed at Scheme 2), present on each kidney (K). Red boxes correlate with higher abundances of proteins while green boxes to lower. Proteins are identified with the respective gene name. The majority of protein present higher abundance values in F1, with the exception of some collagens.

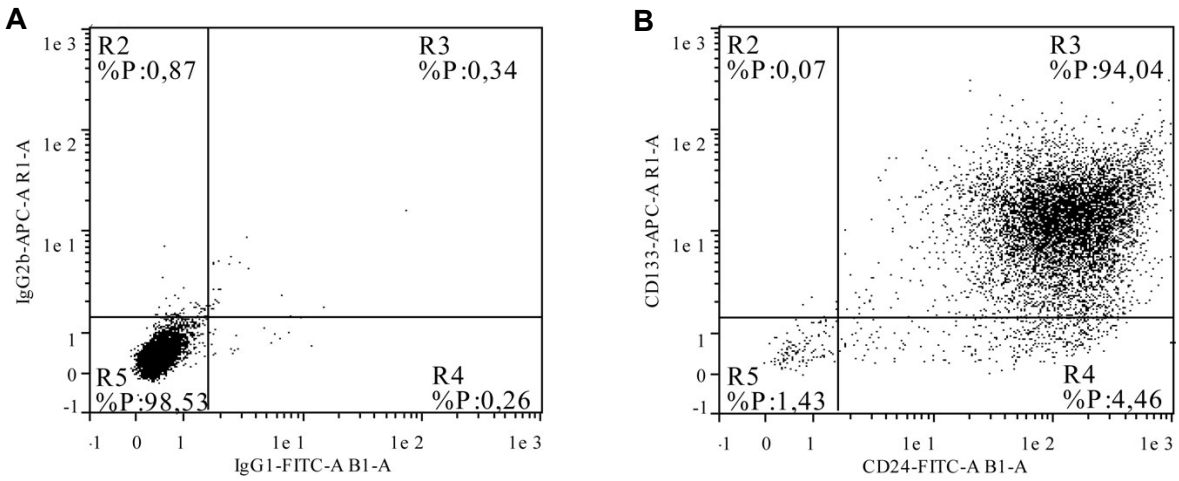

Figure S2 - Flow cytometry characterization of hRPCs. CD133 and CD24 markers expression in human renal progenitor cells confirm that double-positive cells represent a homogeneous population with ~94% double positivity. Images represent (A) Isotype control and (B) double-stained cells.

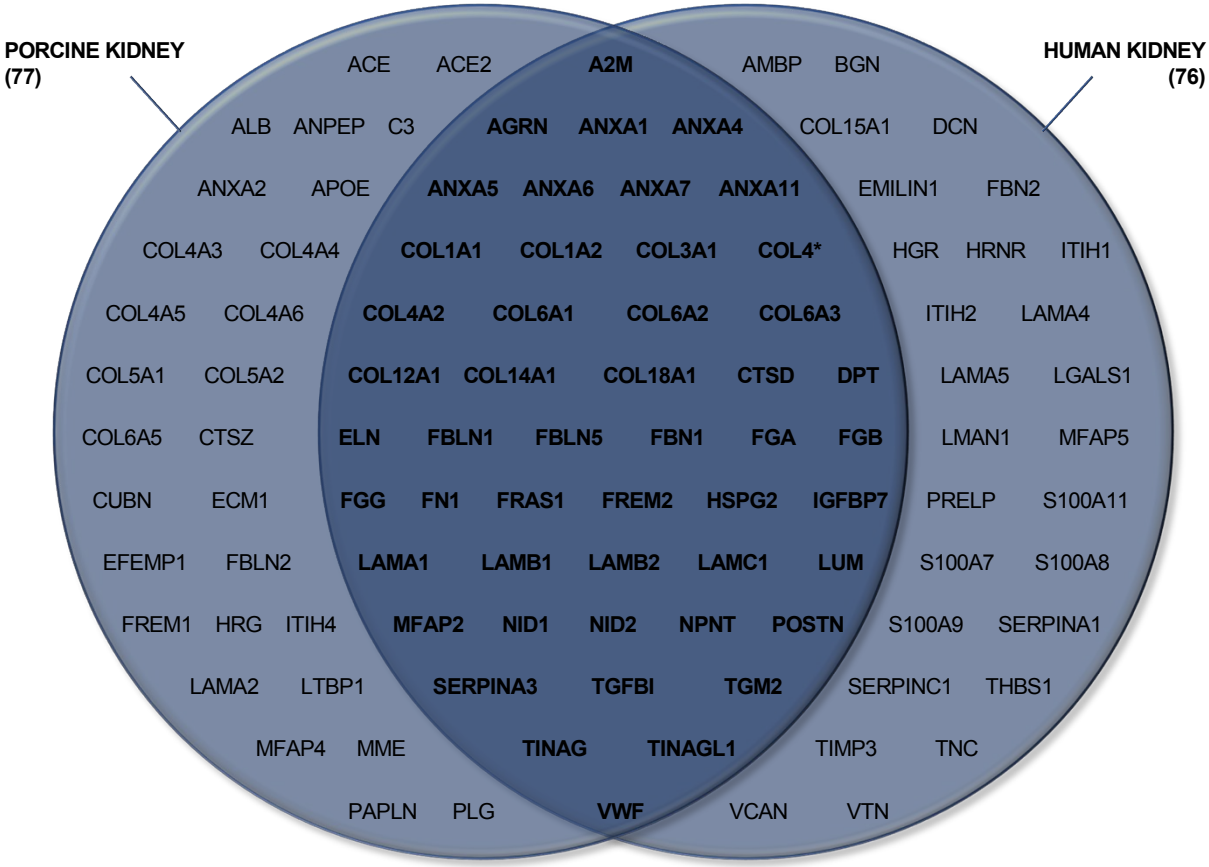

Figure S3 – Venn diagram representing the overlap and differences between the human and porcine kidney ECM proteome as identified by the study of Louzao-martinez et al. Each word represents a single protein that is labeled with the gene name.

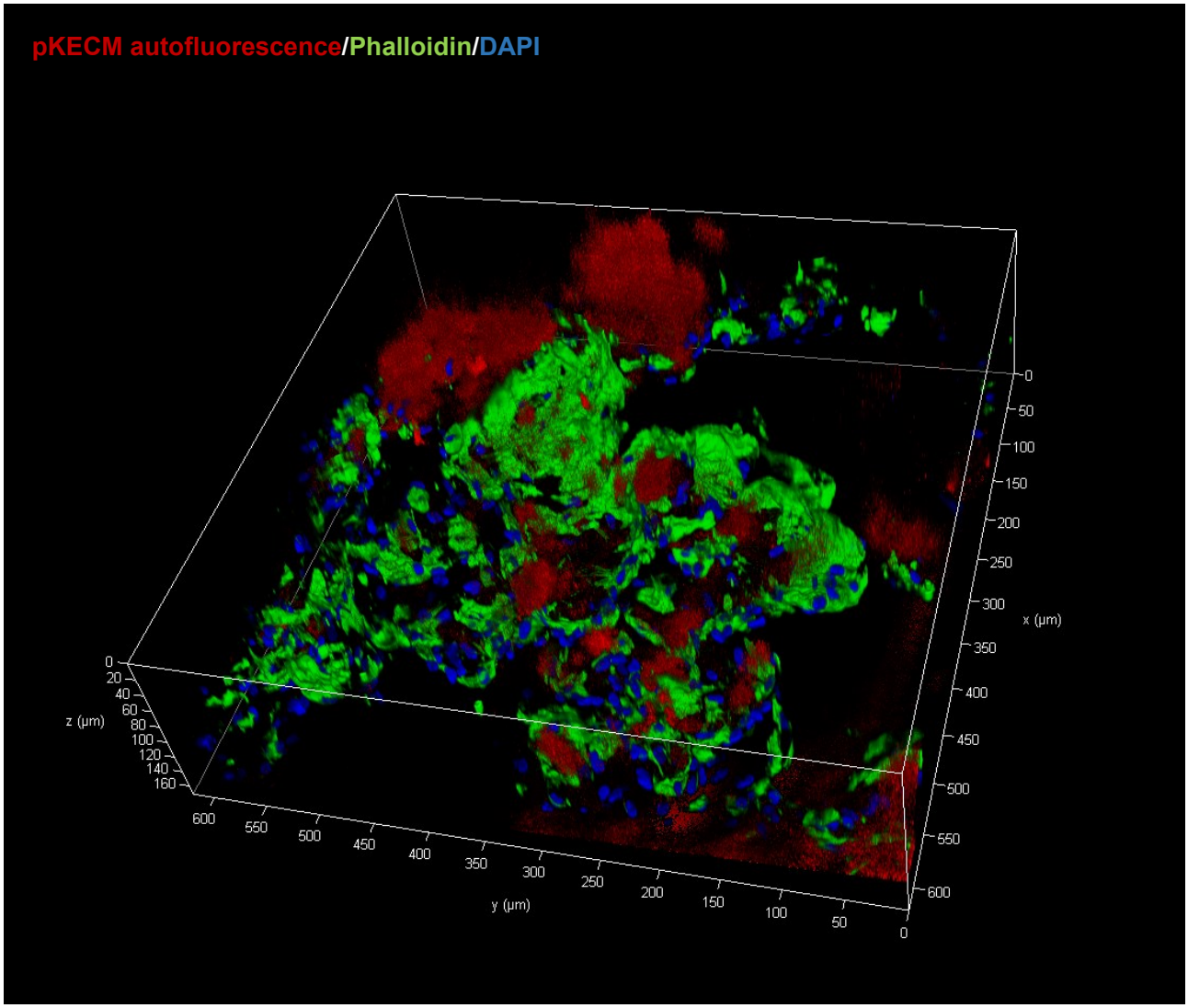

Figure S4 – 3D micrograph of the hRPCs distribution on the pKECM. Immunofluorescence of phalloidin for cytoskeleton (green) and DAPI for nuclei (blue). Matrix autofluorescence appears in red. Numbers are displayed in µm.

Table S1 – Quantitative proteomic analysis of decellularized porcine kidney ECM. Protein description and accession numbers are relative to Sus scrofa database from UniProt. Functional classification was obtained in AmiGO database. The abundance percentage was obtained by dividing each protein abundance to the total abundance of ECM proteins relative to each kidney (K).

Protein	Gene	Accession	Functional Classification	% (vs. Total ECM Proteins)			CV
				K1	K2	K3	
Agrin	AGRN	A0A287AN50	Basement Membrane	0,186	0,199	0,142	0,045
Collagen type XVIII alpha-1 chain	COL18A1	A0A286ZIL9	Basement Membrane	0,010	0,012	0,012	0,325
Similar to Collagen NC1 domain containing protein (IV)	COL4	A0A5G2QEJ2	Basement Membrane	15,738	15,903	5,842	0,313
Collagen alpha-2 (IV) chain	COL4A2	A0A5G2RJ53	Basement Membrane	8,468	7,891	9,799	0,352
Collagen alpha-3 (IV) chain	COL4A3	F1SNP0	Basement Membrane	1,450	1,875	1,089	0,104
Collagen alpha-4 (IV) chain	COL4A4	A0A287BI02	Basement Membrane	0,070	0,085	0,108	0,455
Collagen alpha-5 (IV) chain	COL4A5	A0A287A007	Basement Membrane	1,143	1,025	0,601	0,145
Collagen alpha-6 (IV) chain	COL4A6	F1RXI3	Basement Membrane	0,065	0,077	0,044	0,078
Fraser extracellular matrix complex subunit 1	FRAS1	F1RYS0	Basement Membrane	0,019	0,022	0,021	0,247
FRAS1 related extracellular matrix 1	FREM1	A0A287BGJ4	Basement Membrane	0,004	0,008	0,008	0,453
FRAS1 related extracellular matrix 2	FREM2	F1RS31	Basement Membrane	0,022	0,029	0,045	0,603
Perlecan	HSPG2	A0A287ATP0	Basement Membrane	2,683	2,983	4,180	0,486
Laminin subunit alpha 1	LAMA1	A0A287AG36	Basement Membrane	0,013	0,015	0,012	0,147
Laminin subunit alpha 2	LAMA2	A0A287A027	Basement Membrane	0,008	0,017	0,023	0,669
Laminin beta-1	LAMB1	F1SAE9	Basement Membrane	1,217	1,187	1,049	0,152
Laminin beta-2	LAMB2	A0A287AWV5	Basement Membrane	0,220	0,259	0,567	0,784
Laminin gamma-1	LAMC1	F1S663	Basement Membrane	1,742	2,259	3,520	0,604
Nidogen-1	NID1	F1RGY5	Basement Membrane	1,271	1,520	1,383	0,235
Nidogen-2	NID2	A0A287AKJ2	Basement Membrane	0,103	0,145	0,086	0,142
Nephronectin	NPNT	A0A5G2QQZ6	Basement Membrane	0,055	0,067	0,033	0,143
Papilin, proteoglycan like sulfated glycoprotein	PAPLN	F1S3J7	Basement Membrane	0,013	0,020	0,014	0,201
Aminopeptidase N	ANPEP	A0A5G2QPR2	ECM Regulator	0,076	0,096	1,637	1,559
Inter-alpha-trypsin inhibitor heavy chain H4	ITIH4	A0A286ZN24	ECM Regulator	0,006	0,006	0,053	1,393
Latent transforming growth factor beta binding protein 1	LTBP1	A0A286ZWQ1	ECM Regulator	0,005	0,006	0,011	0,692

Transglutaminase 2	TGM2	A0A5G2R416	ECM Regulator	0,021	0,019	0,190	1,405
Insulin-like growth factor-binding protein 7	IGFBP7	A0A287B8M8	ECM Regulator	0,013	0,009	0,219	1,566
Alpha-2-macroglobulin	A2M	A0A5G2Q8I9	ECM Regulator	0,003	0,004	0,033	1,384
Cathepsin D	CTSD	A0A286ZX26	ECM Regulator	0,000	0,000	0,001	1,529
Cathepsin Z	CTSZ	A5GFX7	ECM Regulator	0,001	0,001	0,005	1,288
Histidine-rich glycoprotein	HRG	F1SFI5	ECM Regulator	0,002	0,002	0,018	1,338
Collagen apha-1 (XII) chain	COL12A1	F1RQI0	FACIT Collagen	1,012	1,311	1,167	0,254
Collagen apha-1 (XIV) chain	COL14A1	A0A287BGV6	FACIT Collagen	0,106	0,137	0,206	0,580
Collagen alpha-1 (I) chain	COL1A1	A0A287A1S6	Fibrillar collagen	35,036	32,737	27,141	0,111
Collagen alpha-2 (I) chain	COL1A2	F1SFA7	Fibrillar collagen	7,601	4,560	6,945	0,387
Collagen alpha-1(III) chain preproprotein	COL3A1	F1RYI8	Fibrillar collagen	1,229	1,249	0,561	0,220
Collagen apha-1 (V) chain	COL5A1	F1S021	Fibrillar collagen	0,026	0,018	0,027	0,408
Collagen apha-2 (V) chain	COL5A2	A0A287BPM1	Fibrillar collagen	0,031	0,037	0,021	0,069
Collagen apha-1 (VI) chain	COL6A1	A0A5G2QW87	Matricellular	5,231	6,294	6,255	0,292
Collagen apha-2 (VI) chain	COL6A2	I3LQ84	Matricellular	3,212	3,923	3,852	0,290
Collagen apha-3 (VI) chain	COL6A3	I3LUR7	Matricellular	3,366	3,965	2,821	0,089
Collagen apha-5 (VI) chain	COL6A5	A0A287BK35	Matricellular	0,680	0,876	1,477	0,651
Dermatopontin	DPT	A0A286ZVB7	Matricellular	0,031	0,034	0,101	0,943
Fibulin 3	EFEMP1	F1SQL2	Matricellular	0,022	0,032	0,047	0,601
Fibulin 1	FBLN1	A0A286ZLN2	Matricellular	0,014	0,015	0,019	0,414
Fibulin 2	FBLN2	A0A287B5Q1	Matricellular	0,003	0,004	0,005	0,477
Fibulin 5	FBLN5	A0A480ZQ94	Matricellular	0,015	0,017	0,002	0,628
Fibrinogen alpha chain	FGA	F1RX36	Matricellular	0,289	0,366	0,566	0,591
Fibrinogen beta chain	FGB	A0A5G2RHA4	Matricellular	1,005	1,229	2,588	0,772
Fibrinogen gamma chain	FGG	F1RX35	Matricellular	0,491	0,631	2,480	1,122
Fibronectin 1	FN1	A0A286ZY95	Matricellular	0,700	0,787	1,137	0,509
Lumican	LUM	F1SQ09	Matricellular	0,038	0,037	0,068	0,619
Periostin	POSTN	A0A5G2R015	Matricellular	0,001	0,002	0,013	1,341
Angiotensin-converting enzyme	ACE	A0A5G2QTW5	Other ECM	0,005	0,006	0,016	0,865

Angiotensin-converting enzyme 2	ACE2	K7GLM4	Other ECM	0,002	0,003	0,034	1,467
Serum albumin	ALB	A0A287BAY9	Other ECM	0,011	0,024	0,059	0,992
Annexin A11	ANXA11	A0A5K1UZZ4	Other ECM	0,005	0,007	0,031	1,205
Annexin A2	ANXA2	A0A5G2QCF9	Other ECM	0,004	0,004	0,015	1,045
Cubilin	CUBN	F1RWC3	Other ECM	0,655	0,832	1,790	0,796
Extracellular matrix protein 1	ECM1	I3LC64	Other ECM	0,003	0,005	0,009	0,747
Neprilysin	MME	A0A287BPD6	Other ECM	0,057	0,071	0,448	1,310
Plasminogen	PLG	P06867	Other ECM	0,114	0,124	0,151	0,387
Annexin A7	ANXA7	F1SU59	Other ECM	0,000	0,001	0,002	0,826
Annexin A4	ANXA4	A0A287AYJ2	Other ECM	0,001	0,001	0,003	1,178
Annexin A5	ANXA5	F2Z5C1	Other ECM	0,000	0,000	0,001	1,350
Annexin A6	ANXA6	A0A5G2RBI3	Other ECM	0,004	0,005	0,019	1,082
Annexin A1	ANXA1	F1SJB5	Other ECM	0,000	0,000	0,003	1,284
Apolipoprotein E	APOE	F1RM45	Secreted	0,001	0,001	0,003	1,044
Complement C3	C3	F1SBS4	Secreted	0,041	0,044	0,162	1,052
Transforming growth factor-beta-induced protein ig-h3	TGFBI	A0A5G2QXN3	Secreted	0,033	0,038	0,059	0,565
von Willebrand factor (Fragment)	VWF	Q28833	Secreted	0,005	0,005	0,004	0,159
SERPIN domain-containing protein	SERPINA3-2	F1SCC6	Secreted	0,000	0,000	0,003	1,732
Elastin	ELN	A0A5G2Q717	Structural ECM	0,022	0,029	0,007	0,469
Fibrillin 1	FBN1	F1SN67	Structural ECM	1,658	1,824	4,354	0,816
Microfibril associated protein 2	MFAP2	F1SUS0	Structural ECM	0,030	0,046	0,087	0,781
Tubulointerstitial nephritis antigen	TINAG	I3L9E7	Structural ECM	2,422	2,730	4,222	0,554
Tubulointerstitial nephritis antigen like 1	TINAGL1	A0A287ANT6	Structural ECM	0,155	0,199	0,268	0,510
Microfibril associated protein 4	MFAP4	A0A287AZP0	Structural ECM	0,001	0,001	0,004	1,168